

## **ADDITIONAL NUMERICAL MODELING DETAILS AND CONSTRAINTS**

Equation 1 is solved using the finite element method with the COMSOL Multiphysics package v3.5a. Relative and absolute tolerances are set to 0.01 and 0.001, respectively. The grid is variably-spaced, with coarser triangular elements in the general domain and fine quadrilateral elements along the newly-intruded sill boundary. In particular, a coarse boundary mesh along the new sill was found to give erroneous calculated volumes, especially in the initial stages of each model, due to averaging along a steep temperature/melt fraction gradient. Therefore, a gradual boundary layer 8 elements wide, with a boundary thickness of  $< 1\text{m}$  is used.

The crystallinity-temperature relationships ( $\chi$ -T) shown in Figure 1a are intended to be general, and aimed at capturing basic trends in assumed compositional inputs to numerical models. The linear trend is a common input in many models, as referenced in the main text. The silicic trend is based on MELTS modeling results (Ghiorso and Sack, 1995) on the Pagosa Peak Dacite by Huber et al. (2009); based on work by Whitney and Stormer (1985) and Bachmann et al. (2002), the Pagosa Peak Dacite, and the Fish Canyon magma suite in general, are generally comparable in major and trace element composition to average granodiorite, and thus to upper continental crust.

Temperature-dependent thermal diffusivity ( $\kappa$ ) is given by Whittington et al. (2009). Following the results of Nabelek et al. (2012), and for simplicity, this dependence is accommodated as a temperature-dependent thermal conductivity by setting  $k_{TD} = \kappa\rho C_p$ . Specific heat capacity was not varied explicitly as a function of temperature. Neglecting this temperature-dependence should have a minor effect compared with varying conductivity, due to the flattening out of specific heat capacity functions at magmatic

temperatures (above ~300 °C; see Nabelek et al., 2012). Nevertheless, in accommodating temperature-dependent thermal properties, residuals in the conservation of energy were explicitly re-calculated:  $(\rho C_p T_t) + (\rho L \frac{\partial X}{\partial T} T_t) - \sqrt{(k_{rr\_htgh} * T_{rr})^2 + (k_{zz\_htgh} * T_{zz})^2}$ , where  $\rho$  and  $C_p$  are constant density and specific heat capacity, listed in Table 1,  $T_t$  is the built-in COMSOL time derivative of temperature,  $T_{rr}$  and  $T_{zz}$  are the built-in COMSOL second space derivatives of temperature, and  $k_{rr\_htgh}$  and  $k_{zz\_htgh}$  are the COMSOL built-in space derivatives of variable conductivity in the general heat transfer module ( $z$  and  $r$  components are the depth and radial modeling components, respectively). The first term above corresponds to the transient term in Equation 1 of the main text; the second term is the change in energy due to latent heat, and the third term is heat diffusion (usually on the right-hand side of the heat equation). Using this calculation, conservation of energy was checked during the cooling (post-intrusion) of one of the models. Residuals were never greater than  $10^{-4}$  W/m<sup>3</sup>; the regions with highest residuals were along material/subdomain boundaries and/or around the edges of the crystallizing magma reservoir.

The initial temperature condition for each new sill is the liquidus temperature (990°C), and for the remaining domain, a geothermal gradient of 30°C/km. Constant temperature boundary conditions are held along the surface (0°C), with insulating and axial boundary conditions along the outer and inner edges (right and left sides of Figure 1c, respectively). The bottom boundary condition is reset at each new sill according to the downdropping/sill insertion procedure described below. When sills are injected, the previously existing crust is down-dropped to make room for the new magma.

Sill thickness was set to 200m for the main results of this study. However, sensitivity tests were run to evaluate the degree to which this thickness, and therefore the time interval between sills defined by the overall modeled emplacement rate, may arbitrarily influence results. We found that our results are independent of sill thickness, which is illustrated in Figure 1A. In this scenario, black lines correspond to the chosen sill

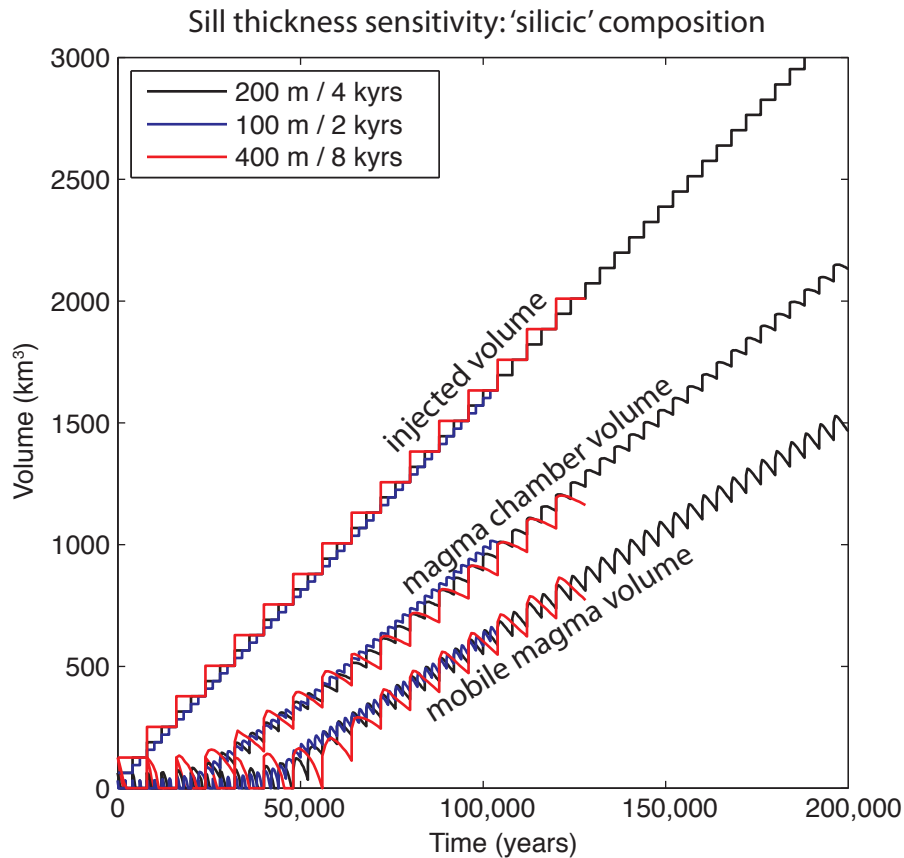


**Figure DR1: Results of sensitivity test to sill interval/thickness variations. Overall emplacement rate is constant, and all models used the 'silicic' composition.**

thickness of 200m, blue lines correspond to half this thickness (100m, and therefore half of the time interval between injections), and red lines to twice this thickness (400m, and therefore twice the time interval between injections). While small differences exist in the

time to accumulation of mobile magma, they are secondary, and the ultimate results and the trends of magma accumulation are independent of assumed sill thicknesses.

Sill insertions are accommodated using the Moving Mesh COMSOL Application Mode. For every model run, sills are 200m in thickness, giving a total stack of 50 sills for each complete run. The time period between sill injections is determined by the sill injection rate. When each new sill is injected, a moving reference frame (*ale*) is translated 200m downwards in subdomains 2 and 3 (see Figure 1). This temperature field is then used to prescribe the initial conditions in the main reference frame (*ref*) of the next inter-sill cooling period for subdomains 1 and 3; subdomain 2 (the new sill) is set to its liquidus temperature. This process is repeated for each new sill.

These models do not consider (1) gas exsolution and convection within the reservoir, and (2) hydrothermal fluid circulation around the growing pluton. Gas exsolution and convective currents within the reservoir could increase the efficiency of magma cooling (particularly if gas can be advected away; Huber et al., 2010); however, these convective processes should have a minimal effect because (1) the majority of magma lifetimes are spent in a mush state which severely limits the efficiency of convective heat transfer (Huber et al., 2009); and (2) the country rock's absorbance and conductance of heat primarily limits heat loss from the intrusion, rather than the intrusion's ability to internally modify its thermal structure (Carrigan, 1988). Hydrothermal fluid circulation could also accelerate cooling at very shallow depths. However, the combination of low permeability surrounding magmatic intrusions and a tendency for hydrothermal systems to become highly overpressured (although this could lead to increased permeability through fracturing) suggests that the role fluids are likely

to play in heat transfer from plutons at depths greater than ~4km is either insignificant, or difficult to quantify generally (Yardley, 2009).

## REFERENCES CITED

- Bachmann, O., Dungan, M. A., and Lipman, P. W., 2002, The Fish Canyon magma body, San Juan Volcanic Field, Colorado: Rejuvenation and eruption of an upper-crustal batholith: *Journal of Petrology*, v. 43, no. 8, p. 1469-1503.
- Carrigan, C. R., 1988, Biot number and thermos bottle effect: Implications for magma-chamber convection: *Geology*, v. 16, p. 771-774.
- Ghiorso, M. S., and Sack, R. O., 1995, Chemical mass transfer in magmatic processes IV. A revised and internally consistent thermodynamic model for the interpolation and extrapolation of liquid-solid equilibria in magmatic systems at elevated temperatures and pressures: *Contrib Mineral Petrol*, v. 119, p. 197-212.
- Huber, C., Bachmann, O., and Manga, M., 2009, Homogenization processes in silicic magma chambers by stirring and mushification (latent heat buffering): *Earth and Planetary Science Letters*, v. 283, no. 1-4, p. 38-47.
- Huber, C., Bachmann, O., and Manga, M., 2010, Two Competing Effects of Volatiles on Heat Transfer in Crystal-rich Magmas: Thermal Insulation vs Defrosting: *Journal of Petrology*, v. 51, no. 4, p. 847-867.
- Nabelek, P. I., Hofmeister, A. M., and Whittington, A. G., 2012, The influence of temperature-dependent thermal diffusivity on the conductive cooling rates of plutons and temperature-time paths in contact aureoles: *Earth and Planetary Science Letters*, v. 317-318, no. C, p. 157-164.
- Whitney, J. A., and Stormer, J. C., 1985, Mineralogy, petrology, and magmatic conditions from the Fish Canyon Tuff, central San Juan volcanic field, Colorado: *Journal of Petrology*, v. 26, p. 726-762.
- Whittington, A. G., Hofmeister, A. M., and Nabelek, P. I., 2009, Temperature-dependent thermal diffusivity of the Earth's crust and implications for magmatism: *Nature*, v. 458, no. 7236, p. 319-321.
- Yardley, B. W. D., 2009, The role of water in the evolution of the continental crust: *Journal of the Geological Society*, v. 166, no. 4, p. 585-600.